ISSN 1070-3284, Russian Journal of Coordination Chemistry, 2013, Vol. 39, No. 10, pp. 716–722. © Pleiades Publishing, Ltd., 2013.

Synthesis, Characterization, Electrochemical Studies, and Antibacterial Activities of Cobalt(III) Complexes with Salpn-Tipe Schiff Base Ligands. Crystal Structure of *trans*-$[Co^{III}(L^1)(Py)_2]ClO_4$[1]

M. Salehi[a, *], M. Kubicki[b], G. Dutkiewicz[b], A. Rezaei[c], M. Behzad[a], and S. Etminani[a]

[a] *Department of Chemistry, College of Science, Semnan University, Semnan, Iran*

[b] *Department of Chemistry, Adam Mickiewicz University, Grunwaldzka 6, Poznan, 60-780 Poland*

[c] *School of Biological Science, Damghan University, Damghan, Iran*

**e-mail: msalehi@sun.semnan.ac.ir*

Received February 24, 2012

Abstract—The synthesis, characterization, spectroscopic and electrochemical properties of *trans*-$[Co^{III}(L^1)(Py)_2]ClO_4$ (**I**) and *trans*-$[Co^{III}(L^2)(Py)_2]ClO_4$ (**II**) complexes, where H_2L^1 = N,N'-bis(5-chloro-2-hydroxybenzylidene)-1,3-propylenediamine and H_2L^2 = N,N'-bis(5-bromo-2-hydroxybenzylidene)-1,3-propylenediamine, have been investigated. Both complexes have been characterized by elemental analysis, FT-IR, UV-Vis, and ^1H NMR spectroscopy. The crystal structure of **I** has been determined by X-ray diffraction. The coordination geometry around cobalt(III) ion is best described as a distorted octahedron. The electrochemical studies of these complexes revealed that the first reduction process corresponding to Co(III/II) is electrochemically irreversible accompanied by dissociation of the axial Co–N(Py) bonds. The in vitro antimicrobial activity of the Schiff bse ligands and their corrsponding complexes have been tested against human pathogenic bacterias such as *Staphylococcus aureus*, *Bacillus subtilis*, *Pseudomonas aeruginosa*, and *Escherichia coli*. The cobalt(III) complexes showed lower antimicrobial activity than the free Schiff base ligands.

DOI: 10.1134/S1070328413100084

INTRODUCTION

Schiff bases are widely used as analytical reagents since they allow simple and inexpensive preparation of a number of organic and inorganic compounds [1]. There is a growing interest in the chemistry of chelate complexes of Schiff bases because of the wide range of applications of these complexes in various fields. Numerous studies are also devoted to the synthesis and characterization of the metal complexes with bioactive organic ligands in order to produce novel potential chemotherapeutic agents. Particularly important is the pressing need for the new antibacterial agents which could replace those losing their effectiveness because of the fast development of microorganisms' resistance [2]. Therefore, the discovery of brand new antimicrobial compounds or finding the ways to increase the effectiveness of previously known drugs is important. Some cobalt complexes with tetradentate Schiff bases are known to exhibit antibacterial activity, amongst their many other applications, such as reversible oxygen transport, potent antiviral or antitumor agents, in enantioselective and asymmetric catalysis, or as the models for vitamin B_{12} [3–8]. In our ongoing studies on the synthesis, structural, spectroscopic and electrochemical studies of cobalt(III) complexes with Schiff base ligands [9, 10], we report here the synthesis and characterization of *trans*-$[Co^{III}(L^1)(Py)_2]ClO_4$ (**I**) and *trans*-$[Co^{III}(L^2)(Py)_2]ClO_4$ (**II**) complexes. Their spectral properties were investigated by FT-IR, UV-Vis, and ^1H NMR spectra. The X-ray crystal structure of **I** has been determined. Electrochemical properties of these complexes are reported and discussed. Antibacterial activities of the Schiff base ligands and their complexes against *Bacillus subtilis* (Gram-positive), *Staphylococcus aureus* (Gram-positive), *Escherichia coli* (Gram-negative), and *Pseudomonas aeruginosa* (Gram-negative) are investigated for the first time.

EXPERIMENTAL

Materials and methods. All solvents and chemicals were used as received, except the amines which were distilled under reduced pressure prior to use. Elemental analyses were performed by using a PerkinElmer 2400II CHNS-O elemental analyzer. ^1H NMR spec-

[1] The article is published in the original.

tra were recorded on a 500 MHz Bruker FT-NMR spectrometer using $CDCl_3$ solvent; chemical shifts (δ) are given in ppm. IR spectra were obtained as KBr plates using a Bruker FT-IR instrument and UV-Vis spectra were obtained on a Shimadzu UV-1650PC spectrophotometer. A Metrohm 757 VA computerace instrument was employed to obtain cyclic voltammograms in acetonitrile at room temperature (25°C) using 0.1 M tetra-*n*-butylammonium hexafluorophosphate solution as supporting electrolyte.

Synthesis of Schiff base ligands. The Schiff base ligands, N,N'-bis(5-chloro-2-hydroxybenzylidene)-1,3-propylenediamine (**H_2L^1**) and N,N'-bis(5-bromo-2-hydroxybenzylidene)-1,3-propylenediamine (**H_2L^2**), were prepared as described in [11].

Synthesis of complex I. $Co(CH_3COO)_2 \cdot 4H_2O$ (0.125 g, 0.5 mmol), dissolved in 10 mL of methanol, was added to a methanolic solution (20 mL) of H_2L^1 (0.175 g, 0.5 mmol) with constant stirring. To the resulting solution was added 4 mmol of pyridine, and air was bubbled through the reaction mixture for about 3 h. Then 0.5 mmol of $NaClO_4$ was added to the resulting brown solution and stirred for 5 min. A brown microcrystalline solid was produced by slow evaporation of methanol at room temperature. The precipitate was washed with and redissolved in methanol. The single crystals suitable of compound **I** were obtained by slow evaporation of the methanol solution of this compound after 3 days. The crystals were filtered off and washed with a small amount of cold methanol and dried under vacuum. The yield of **I** was 50%.

For $C_{27}H_{24}N_4O_6Cl_3Co$			
anal. calcd., %:	C, 48.71;	H, 3.63;	N, 8.42.
Found, %:	C, 48.50;	H, 3.58;	N, 8.35.

FT-IR (KBr; ν, cm^{-1}): 1609 (C=N), 1082 (Cl–O) UV-Vis (CH_3CN; λ_{max}, nm (ε, L mol^{-1} cm^{-1})): 226 (59300), 250 (48300), 392 (6990), 575 (380). ^1H NMR. (500 MHz; $CDCl_3$; δ, ppm): 1.30 (s., $2H_a$), 3.87 (m., $4H_b$), 7.02–7.40 (m., 10H, Ar), 8.45 (s., $2H_c$).

Synthesis of complex II. The complex was prepared by the same method as for **I** except that H_2L^2 was used instead of H_2L^1. The compound recrystallised from methanol, but no suitable single crystals were grown for complex **II**. The yield was 55%.

For $C_{27}H_{24}N_4O_2Br_2Co$			
anal. calcd., %:	C, 68.20;	H, 5.72;	N, 9.94.
Found, %:	C, 68.05;	H, 5.65;	N, 9.78.

FT-IR (KBr; ν, cm^{-1}): 1618 (C=N), 1084 (Cl–O) UV-Vis (CH_3CN; λ_{max}, nm (ε, L mol^{-1} cm^{-1})): 224 (58500), 251 (47400), 329 (6570), 575 (381). ^1H NMR. (500 MHz; $CDCl_3$; δ, ppm): 1.23 (s., $2H_a$), 3.79 (m., $4H_b$), 7.05–7.78 (m., 10H, Ar), 8.36 (s., $2H_c$).

X-ray structure determination. Diffraction data of complex **I** were collected at room temperature by the ω-scan technique on an Agilent Technologies Xcalibur four-circle diffractometer with Eos CCD-detector and graphite-monochromatized MoK_α radiation source (λ = 0.71073 Å). The data were corrected for Lorentz-polarization as well as for absorption effects [12]. Precise unit-cell parameters were determined by a least-squares fit of 30159 reflections of the highest intensity, chosen from the whole experiment. The structure was solved with SIR92 [13] and refined with the full-matrix least-squares procedure on F^2 by SHELXL-97 [14]. The scattering factors incorporated in SHELXL-97 were used. The function $\Sigma w(|F_o|^2 - |F_c|^2)^2$ was minimized, with $w^{-1} = [\sigma^2(F_o)^2 + (0.0840P)^2 + 3.2183P]$ ($P = [\mathrm{Max}(F_o^2, 0) + 2F_c^2]/3$) [14]. All non-hydrogen atoms were refined anisotropically, the hydrogen atoms were placed geometrically in idealized positions and refined as rigid groups with their U_{iso}'s as 1.2 or 1.5 (methyl) times U_{eq} of the appropriate carrier atom. The large residual electron density has been interpreted as the half-occupied solvent (methanol) molecule, which did not interact specifically with the rest of the structure. Hydrogen atoms from this molecule have not been found and no attempts to determine their positions have been performed. Relevant crystal data are listed in Table 1 together with refinement details. A full detail of data collections and structure determinations has been deposited with the Cambridge Crystallographic Data Centre (146366 (**I**); deposit@ccdc.cam.ac.uk or http://www.ccdc.cam.ac.uk).

Bacterial strains. The metal complexes and ligands were individually tested against a penal of microorganisms (Gram negative and Gram positive), namely *Bacillus subtilis* (*B. subtilis*; PTCC no. 1023; ATCC 6633); *Staphylococcus aureus* (*S. aureus*; PTCC no. 1431; ATCC 25923), *Escherichia coli* (*E. coli*; PTCC no. 1399; ATCC 25922), and *Pseudomonas aeruginosa* (*P. aeruginosa*; PTCC no. 1430; ATCC 27853). The organisms were purchased from Iranian Research Organization for Science and Technology (IROST).

Disc diffusion assay. Single-disk diffusion as a qualitative assay was performed according to Bauer et al. [15]. Briefly, four to five colonies of each organism were inoculated into 4 ml of broth and incubated for 4 to 6 h at 37°C. A suspension of each organism was then standardized against a turbidity standard of 0.5 McFarland [16]. Bacteria were cultured on to agar plates using a sterile absorbent cotton swabs. Then plates were incubated at 35°C and the zones of inhibition were measured after 24 h. Each organism was tested in duplicate on different days to measure the reproducibility of the test. Ampicillin (10 мg/disc),

Chloramphenicol (30 мg/disc), and Kanamycin (30 мg/disc), purchased from PadtanTeb Company (Iran), were used as reference antibacterial agents. A set of assay tubes containing only inoculated medium was kept as negative control and likewise solvent controls were also done simultaneously. All assays were performed in duplicate.

Minimum inhibitory concentration (MIC) of chemicals were determined by the broth twofold dilution method as a quantitative assay [17]. Briefly, serial diluted chemical compounds in the range of 0.04–0.29 mg/mL were added to a final inoculum of approximately 1.5×10^6 organisms per ml in log phase growth. The cultures were incubated on a rotary shaker at 37°C for 24 h. MIC (mg/mL) of each tested compounds were defined as the lowest concentration exhibiting no visible growth compared with the drug-free control wells. Each organism was tested in duplicate on different days to measure the reproducibility of the test.

Minimal bactericidal concentration (MBC). To measure MBC, 100 μL volumes of all clear (no growth) tubes from a dilution MIC test was spread on to separate agar plates and incubated at 37°C for 24 h. The MBC (mg/mL) was defined as the lowest concentration of the complex that no growth occurred.

RESULTS AND DISCUSSION

The complexes **I** and **II** were synthesized by reactions of the corresponding ligands, H_2L^1 and H_2L^2, with cobalt(II) acetate in the presence of pyridine in aerobic conditions to acordind the following scheme:

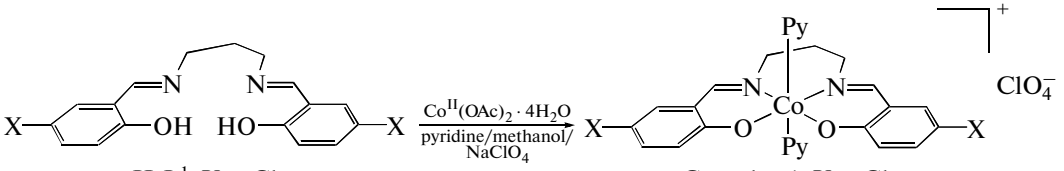

H_2L^1: X = Cl
H_2L^2: X = Br

Complex 1: X = Cl
Complex 2: X = Br

The air oxidation was continued for a period of 3 h, during which the color of the solution changed from brown to green. The diamagnetic character of the complexes indicated that the cobalt atom in both cases had a low spin d^6 conguration and +3 oxidation state. The elemental analysis data of the complexes **I** and **II** are in good agreement with the calculated values.

The IR spectra of the free Schiff base ligands and corresponding complexes show several bands in the 400–4000 cm^{-1} region. The OH stretching frequency of the ligands is observed in the region of 3000–3100 cm^{-1} is due to the internal hydrogen bonding vibration (O–H···N). The disappearance of this band in the FT-IR spectra of the complexes confims that the tetradentate ligands coordinate in their deprotonated forms [18, 19]. The ν(C=N) bands appearing at 1610 cm^{-1} in H_2L^1 and 1614 cm^{-1} in H_2L^1 are shifted to lower frequencies by about 16–27 cm^{-1} in the corresponding cobalt complexes, indicating that the ligands are coordinated to the metal ions through the nitrogen atoms of the azomethine groups [20]. The stretching vibration of ClO_4^- anion appears at 1082 cm^{-1} in **I** and at 1084 cm^{-1} in **II** [21].

The electronic absorption spectra of the free ligands and their corresponding complexes are measured in acetonitrile. The electronic absorption spectra of H_2L^1 and H_2L^2 show a band at 415 and 326 nm attributed to $n \rightarrow p^*$ and $p \rightarrow p^*$ transitions of azomethine chromophore respectively. The two bands in the higher energy regions, at 222 and 253 nm, are attributed to $p \rightarrow p^*$ transitions of the benzene ring [22–24]. The $n \rightarrow p^*$ bands are absent in the spectra of the cobalt complexes. In addition, the intraligand $p \rightarrow p^*$ transitions are red shifted by 66 nm in the corresponding Co(III) complexes presumably due to the increased conjugation after coordination with the metal ion [25]. The appearance of an additional new shoulder at 575 nm in the spectra of Co(III) complexes is attributed to a *d–d* transition.

The ^{1}H NMR spectral data are presented in the experimental section. An octahedral *trans*-structure for **II** can be inferred based on the similarity of the ^{1}H NMR spectra of this complex with that of complex **I**. The signals due to the aliphatic protons of the propylene chelate ring have been observed as a multiplet and a triplet (1 : 2 ratio) at 1.30 (H_a) and 3.87 ppm (H_b) in **I** and at 1.23 (H_a) and 3.79 ppm (H_b) in **II**, respectively. The signals due to the aromatic protons of the phenyl rings and those of the axial (Py) amine as complex multiplets located between 7.02 and 8.40 ppm in **I**, between 7.05 and 8.36 ppm in **II**.

The cyclic voltammetry data of the complexes were recorded at room temperature under nitrogen atmosphere, in acetonitrile solution containing 0.1 M TBAH as supporting electrolyte. The electrochemical data of two complexes are summarized in Table 2 (versus Ag/AgCl reference electrode), and Fig. 1 shows the cyclic voltammogram of representative complex **I**. The first electrochemically irreversible reduction process at –0.425 V is attributed to the following reaction (Eq. (1)):

Table 1. Crystal data, data collection and structure refinement of structure I

Parameter	Value
Chemical formula	$[(C_{27}H_{24}Cl_2CoN_4O_2)](ClO_4)\cdot 1/4(CH_3OH)$
Formula weight	672.79
Crystal system	Triclinic
Space group	$P\bar{1}$
a, Å	11.732(1)
b, Å	15.803(2)
c, Å	16.664(2)
α, deg	75.30(2)
β, deg	87.55(2)
γ, deg	83.11(2)
V, Å^3	2966.6(6)
Z	4
ρ_{calcd}, g cm^{-3}	1.506
$F(000)$	1374
μ, mm^{-1}	0.901
θ Range, deg	3.0–29.0
Limiting indices h, k, l	$-15 \le h \le 15$, $-21 \le k \le 21$, $-21 \le l \le 22$
Reflections collected/unique (R_{int})	64661/14275 (0.029)
Reflections with $I > 2\sigma(I)$	11038
Parameters	764
Final R index ($I > 2\sigma(I)$)	$R_1 = 0.0488$, $wR_2 = 0.1406$
R index (all data)	$R_1 = 0.0679$, $wR_2 = 0.1577$
Goodness-of-fit on F^2	0.99
$\Delta\rho_{max}/\Delta\rho_{min}$, e Å^{-3}	1.10/–0.70

$$trans\text{-}\left[Co^{III}(L^1)(Py)_2\right]^+ + e^- \rightarrow \left[Co^{II}(L^1)\right] + 2Py. \quad (1)$$

The lack of reversibility is likely due to the loss of the ligands from the Co(II) complex because the electron is added to antibonding d_z^2 orbital [20, 26]. The second electrochemically irreversible reduction couple observed at –1.58 V (ΔE = 165 mV) is related to the following one-electron transfer process (Eq. (2)):

$$\left[Co^{II}(L^1)\right] + e^- \rightarrow \left[Co^{I}(L^1)\right]^-. \quad (2)$$

The electrochemical behaviour of complex **II** is similar to that observed for **I**. As shown in Table 2, the redox potentials in **II** complex are shifted to more negative values relative to that observed in **I**, which demonstrates the more electron-withdrawing ability of Cl^- substituent's in L^1 ligand relative to Br^- in L^2 ligand.

Figure 2 gives perspective view of the asymmetric unit of complex **I.** The solid state form of complex **I** is a disordered solvate (**I** · Solv), where Solv is most likely a partially occupied methanol molecule that appeared to be hydrogen bonded to symmetry-related methanol molecule at O···O distances of 2.92 Å. Selected bond lengths and angles are given in Table 3. Two independent $[Co^{III}(L^1)(Py)_2]^+$ cations and two ClO_4^- anions are held together essentially via electrostatic interactions and hydrogen bonds. The cobalt atom exhibited a distorted octahedral stereochemistry. The H_2L^1 ligand is coordinated in the equatorial plane by N_2O_2 system and shows a cisoid conformation. The interplanar angle of the two phenyl rings was 48.7° and the conformation of the equatorial moiety could be described as an asymmetric umbrella. Two pyridine molecules attached to the metal atom via their nitrogens filled its axial sites and adopted a mutually perpendicular disposition with a dihedral angle of 84.95(17)°. The distances between the cobalt atom and the two axial nitrogen donor atoms differed only slightly (1.964(2) and 1.972(2) Å) and compared well with the Co–N distances found in cobalt-ammine complexes, e.g. $[Co(NH_3)_6]Cl_3$ (Co–N = 1.963 Å), *trans*-$[Co(Salen)(Py)_2][BPh_4]$ (**III**) (Co–N = 1.955 Å) and $[Co(3\text{-Cl-Acacen})(NH_3)_2]BPh_4$ (Co–N = 1.955 Å) [26, 27]. The average Co–O distance (1.899(2) Å) and the O(1*A*)–Co–O(15*A*) angle (84.03(9)°) compared well with those reported for **III** (1.884 Å and 85.8°, respectively) [28]. The average Co–N_{eq} distance (1.944 Å) was considerably longer than that of **III** (1.888 Å) and the N(8*A*)CoN(12*A*) angle (94.06(11)°) was larger than the corresponding angle in the related Salen complex (85.5(2)°) [28]. In the crystal structure the Co complexes were arranged in undulating infinite layers parallel to (010) with the ClO_4 anions and the

Table 2. Redox potentials of cobalt complexes in acetonitrile*

Complex	E_{pc1}	E_{pa1}	E_{pc2}	E_{pa2}
trans-$[Co^{III}(L^1)(Py)_2]ClO_4$	–0.425	0.763	–1.58	–1.400
trans-$[Co^{III}(L^2)(Py)_2]ClO_4$	–0.429	0.721	–1.65	–1.405

* Potentials are in 0.1 M TBAH, T = 298 K. Scan rate is 100 mV s^{-1}. Approximate concentrations is 4×10^{-3}–10^{-5} mol/L.

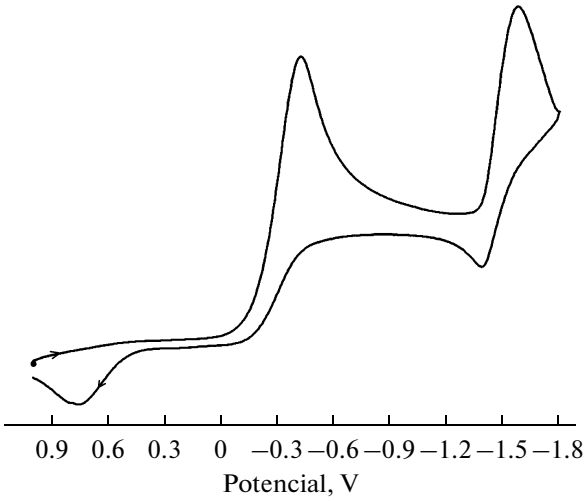

Fig. 1. Cyclic voltammogram of *trans*-$[Co^{III}(L^1)(Py)_2]ClO_4$ in acetonitrile solution at 298 K. Scan rate = 100 mV/s. $c = 4.0 \times 10^{-4}$ mol/L.

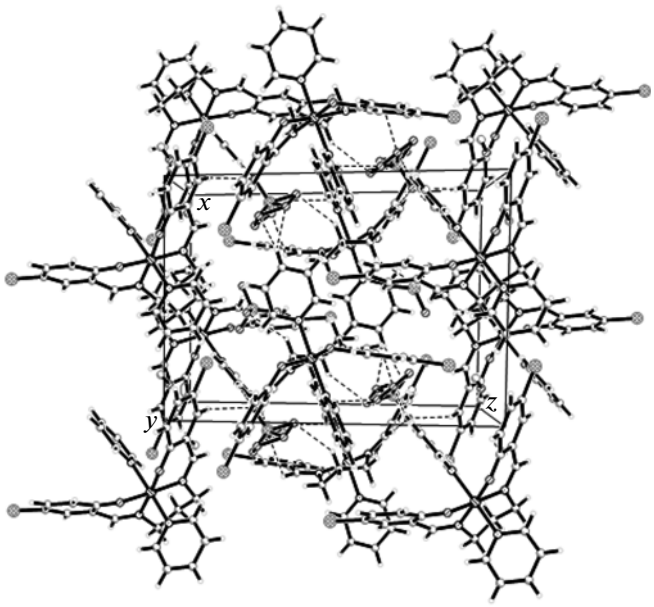

Fig. 3. The crystal packing of **I** as seen along [010] direction. The dashed lines denote hydrogen bonds.

disordered substoichiometric solvent located between the layers (Fig. 3). The crystal packing was mainly determined by electrostatic coulombic interaction between the charged elements of the structure, although some weak but directional C–H···O hydrogen bonds (Table 4) also connected cations and anions.

Others reported previously that the presence of electron withdrawing and electron donating substituents on the Schiff bases ligands has a direct influence on the antibacterial activity of these ligands and their corresponding complexes [29]. Table 5 shows the antibacterial activity results of both Schiff bases ligands and corresponding complexes and also ampicillin, chloramphenicol and Kanamycin as a standard compounds, evaluated by Kirby–Bauer disc diffusion method and serial dilution sensitivity test against both Gram-positive and Gram-negative bacteria. Even the ligands show lower antibacterial activity compared to the standards, but all the ligands are more active than their respective metal complexes. Except *P. aeruginosa* which shows complete resistance through all assays, other studied strains showed slight susceptibility to chemical compounds. According to CLSI interpretive criteria [30], in disc diffusion assay *S. aureus* (Gram-positive) and *E. coli* (Gram-negative) both were susceptible to H_2L^1 and H_2L^2 while their susceptibility to complexes were intermediate. Also, *B. subtilis* (Gram-positive) showed intermediate susceptibility to H_2L^1 and H_2L^2 but was resistant to complexes. Collectively H_2L^1 and H_2L^2 had most antibacterial activities in qualitative disc diffusion assay. Our results showed that H_2L^2 had most inhibitory effects (MIC 0.07 mg/mL) in both studied Gram-positive strains as the same for H_2L^1 and complex **II** in *S. aureus* and *B. subtilis,* respectively. H_2L^2 showed also most inhibitory effects (MIC 0.07 mg/mL) in Gram-negative *E. coli*. Although, regarding to CLSI breakpoint criteria [30] all strains may be considered resistance to these chemicals (MIC ≥ 0.032 mg/mL). Minimal bactericidal concentration of H_2L^2 in *B. subtilis* was the same as

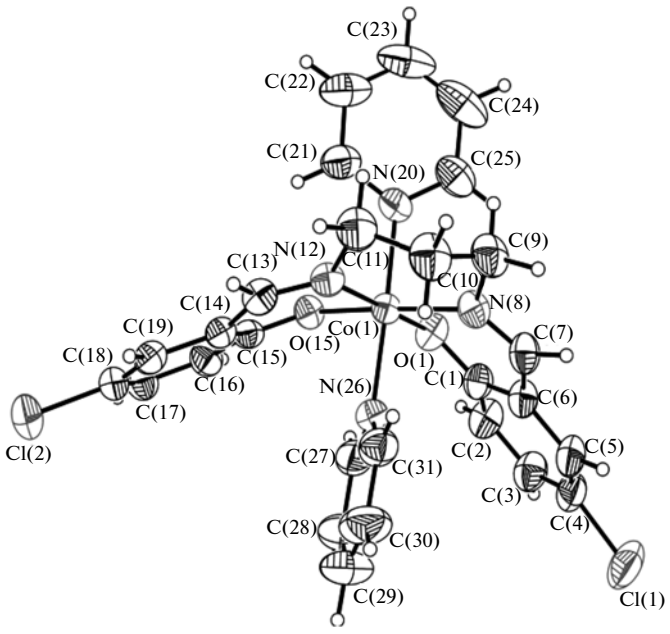

Fig. 2. Perspective view of the cation 1A with labelling scheme. Displacement ellipsoids are drawn at 50% probability level; hydrogen atoms are depicted as spheres of arbitrary radii. Perchlorate anion and disordered solvent (methanol) molecule have been omitted for clarity.

Table 3. Selected bond lengths (Å) and angles (deg) for compound **I**

Bond	*d*, Å
Co(1*A*)–O(1*A*)	1.902(2)
Co(1*A*)–O(15*A*)	1.896(2)
Co(1*A*)–N(8*A*)	1.941(3)
Co(1*A*)–N(12*A*)	1.947(2)
Co(1*A*)–N(20*A*)	1.964(2)
Co(1*A*)–N(26*A*)	1.972(2)
Angle	**w, deg**
O(1*A*)Co(1*A*)O(15*A*)	84.0(9)
O(1*A*)Co(1*A*)N(8*A*)	90.1(11)
O(1*A*)Co(1*A*)N(12*A*)	175.7(10)
O(1*A*)Co(1*A*)N(20*A*)	88.7(11)
O(1*A*)Co(1*A*)N(26*A*)	90.7(11)
O(15*A*)Co(1*A*)(N8*A*)	174.0(10)
O(15*A*)Co(1*A*)(N12*A*)	91.9(10)
O((15*A*)Co(1*A*)(N20*A*)	88.5(10)
O(15*A*)Co(1*A*)(N26*A*)	88.7 (10)
N(8*A*)Co(1*A*)(N12*A*)	94.0 (11)
N(8*A*)Co(1*A*)(N20*A*)	92.4 (11)
N(8*A*)Co(1*A*)(N26*A*)	90.4 (11)

Table 4. Geometric parameters of hydrogen bonds in *trans*-$[Co^{III}(L^1)(Py)_2]ClO_4$*

Contact D–H···A	Distance, Å			Angle DHA, deg
	D–H	H···A	H···A	
C(9*A*)H(9*A*1)O(43)^{i}	0.97	2.57	3.377(7)	140
C(5*B*)H(5*B*)O(31)^{i}	0.93	2.53	3.338(4)	146
C(7*A*)H(7*A*)O(31)^{ii}	0.93	2.48	3.399(3)	170
C(10*A*)H(10*B*)O(34)	0.97	2.55	3.399(4)	146
C(13*A*)H(13*A*)O(32)	0.93	2.43	2.888(4)	110
C(21*A*)H(21*A*)O(15*A*)	0.93	2.53	2.902(4)	104
C(23*A*)H(23*A*)O(33)^{i}	0.93	2.38	3.228(5)	151
C(23*B*)H(23*B*)O(32)^{iii}	0.93	2.54	3.323(5)	142
C(24*B*)H(24*B*)O(31)^{iii}	0.93	2.48	3.345(4)	154
C(29*B*)H(29*B*)O(15*B*)^{iv}	0.93	2.49	3.071(4)	121

* Symmetry codes: ^{i} $1-x, 1-y, 1-z$; ^{ii} $-x, 1-y, 1-z$; ^{iii} $1+x, y, -1+z$; ^{iv} $1-x, 2-y, -z$.

Table 5. Zones of inhibition, MICs and MBCs of antibacterial compounds against pathogenic bacteria

Human pathogenic bacterias	Zones of inhibition, mm*						
	I	**II**	H_2L^1	H_2L^2	Ampicillin (10 mg/disc)	Chloramphenicol (30 mg/disc)	Kanamycin (30 mg/disc)
Bacillus subtilis	12	14	19	16	22	26	21
Staphylococcus aureus	14	17	25	22	29	24	20
Escherichia coli	10	12	25	20	15	21	15
Pseudomonas aeruginosa							

Human pathogenic bacterias	MIC** and MBC***, mg/mL							
	I		**II**		H_2L^1		H_2L^2	
	MIC	MBC	MIC	MBC	MIC	MBC	MIC	MBC
Bacillus subtilis	0.22	0.22	0.07	>0.29	0.15	0.15	0.07	0.07
Staphylococcus aureus	0.27	>0.29	0.15	0.27	0.07	0.17	0.07	0.17
Escherichia coli	0.22	>0.29	0.2	0.25	0.07	0.15	0.15	0.15
Pseudomonas aeruginosa								

* Concentration of 30 mg/mL of each chemical compound was used for disc diffusion assay.

** MIC, minimal inhibitory concentration.

*** MBC, minimal bacterial concentration.

MIC (0.07 mg/mL) while MBCs of H_2L^1 and H_2L^2 in *S. aureus* and *E. coli* were about twofold higher than the corresponding MICs. H_2L^1 and H_2L^2 showed higher antibacterial activities compared to their complexes. In addition, it seems that H_2L^1 and H_2L^2 had similar inhibitory effects in quantitative and qualitative antibacterial assays in studied Gram-positive and Gram-negative strains. However, the susceptibility of *B. subtilis* to these compounds was more than others.

Potent antibacterial activity of cobalt(II) and cobalt(III) Schiff base complexes have been reported in different studies [6, 29, 31]. In disc diffusion method the diameter of the zone is related to the susceptibility of the isolate and to the diffusion rate of the drug through the agar medium [32]. Dipole moment, solubility, molecular mass and hydrophobicity of chemical compounds may affect on their diffusion rate on agar plates. Besides, stability of the chemicals structure has possibly important role in their antibacterial activities. According to MIC and MBC measurements in our study, antibacterial activity of Schiff base ligands was more than their complexes. Although, the antibacterial activity of the metal complexes has been reported more than their respective Schiff bases [6, 29, 31], the Schiff bases are, in a few cases, more active than the metal complexes [31, 33]. The moderate antibacterial activity of the Schiff bases may arise from the presence of imine groups and also from the presence of the hydroxyl groups because of their capacity of hydrogen bonding interactions with cellular compartment. Many factors such as chelation/coordination of the metal ion, solubility, dipole moment and conductivity influenced by the metal ion may be the possible reasons for the antibacterial activities of these metal complexes [34]. But the decrease of the electron densities by the coordination through the donor atoms may cause a decrease of the activities of the complexes [35]. To clear that antibacterial activity of chemical compounds influence DNA structure, interfere with replication, transcription, translation and other biological systems need more researches.

ACKNOWLEDGMENTS

We thank Semnan University for supporting this study. We are grateful to Hamid Nooshiri for excellent technical assistance during the early part of this work.

REFERENCES

1. Cimernman, Z., Galic, N., and Bosner, B., *Anal. Chim. Acta,* 1997, vol. 343, p. 145.
2. Leeb, M., *Nature*, 2004, vol. 431, p. 892.
3. Patil, S.A., Naik, V.H., Kulkarni, A.D., and Badami, P.S., *J. Mol. Struct.*, 2011, vol. 985, p. 330.
4. Yamada, S., *Coord. Chem. Rev.*, 1999, vols. 190–192, p. 537.
5. Bianchini, C. and Zoeliner, R.W., *Adv. Inorg. Chem.*, 1997, vol. 44, p. 263.
6. Zhu, Y. and Li, W.-H., *Transition Met. Chem.*, 2010, vol. 35, p. 745.
7. Amirnasr, M., Shenk, K.J., Gorji, A., and Vafazadeh, R., *Polyhedron*, 2001, vol. 20, p. 695.
8. Zhang, Y.L., Ruan, W.J., Zhao, X.J., et al., *Polyhedron*, 2003, vol. 22, p. 1535.
9. Salehi, M., Dutkiewicz, G., and Kubicki, M., *Acta Crystallogr., E*, 2010, vol. 66, p. 1590.
10. Schenk, K.J., Meghdadi, S., Amirnasr, M., et al., *Polyhedron*, 2007, vol. 26, p. 5448.
11. Elerman, Y., Elmali, Y., Kabak, M., and Svoboda, I., *Acta Crystallogr., C,* 1998, vol. 54, p. 1701.
12. Agilent Technologies, CRYSALIS PRO, Version 1.171.33.36d, Oxford Diffraction Ltd., 2010.
13. Altomare, A., Cascarano, G., Giacovazzo, C., and Gualardi, A., *J. Appl. Crystallogr.*, 1993, vol. 26, p. 343.
14. Sheldrick, G.M., *Acta Crystallogr., A*, 2008, vol. 64, p. 112.
15. Bauer, A.W., Kirby, W.M., Sheris, J.C., and Turck, M., *Am. J. Clin. Pathol.*, 1966, vol. 45, p. 493.
16. Goldman, E. and Green, L.H., *Practical Handbook of Microbiology,* New York: CRC Press, Taylor & Francis Group, 2009, p. 37.
17. European Committee for Antimicrobial Susceptibility Testing (EUCAST) of the European Society of Clinical Microbiology and Infectious Diseases (ESCMID), *Clin. Microbiol. Infect.,* 2000, vol. 6, p. 509.
18. Anthonysamy, A. and Balasubramanian, S., *Inorg. Chem. Commun.*, 2005, vol. 8, p. 908.
19. Garg, B.S. and Kumar, D.N., *Spectrochim. Acta, A*, 2003, vol. 59, p. 229.
20. Amirnasr, M., Vafazadeh, R., and Mahmoudkhani, A., *Can. J. Chem.*, 2002, vol. 80, p. 1196.
21. Nakamoto, K., *Infrared Spectra of Inorganic Compounds,* New York: Wiley, 1970.
22. Zamian, J.R. and Dockal, E.R., *Transition Met. Chem.*, 1996, vol. 21, p. 370.
23. Felicio, R.C., da Silva, G.A., Ceridorio, L.F., and Dockal, E.R., *Synth. React. Inorg. Met. Org. Chem.*, 1999, vol. 29, p. 171.
24. Signorini, O., Dockal, E.R., Castellano, G., and Oliva, G., *Polyhedron*, 1996, vol. 15, p. 245.
25. Zhang, Y.-L., Ruan, W.-J., Zhao, X.-J., et al., *Polyhedron*, 2003, vol. 22, p. 1535.
26. Bottche, A., Takeuchi, T., Hardcastle, K.I., et al., *Inorg. Chem.*, 1997, vol. 36, p. 2498.
27. Kruger, G.J. and Reynhardt, E.C., *Acta Crystallogr.*, *B*, 1978, vol. 34, p. 915.
28. Shi, X.-H., You, X.-Z., Li, C., et al., *Acta Crystallogr., C*, 1995, vol. 51, p. 206.
29. Nejo, A.A., Kolawole, G.A., and Nejo, A.O., *J. Coord. Chem.*, 2010, vol. 63, p. 4398.
30. Performance Standards for Antimicrobial Susceptibility Testing, M100–S19, Wayne (PA, USA): Clinical and Laboratory Standards Institute, 2009.
31. Mishra, A., Kaushik, N.K., Verma, A.K., and Gupta, R., *Eur. J. Med. Chem.*, 2008, vol. 43, p. 2189.
32. Jorgensen, J.H. and Ferraro, M.J., *Clin. Infect. Dis.*, 2009, vol. 49, p. 1749.
33. Özdemir, Ü.Ö., Arslan, F., and Hamurcu, F., *Inorg. Chim. Acta,* 2009, vol. 362, p. 2613.
34. Chohan, Z.H., Hassan, M.U., Khan, K.M., and Supuran, C.T., *J. Enzym. Inhib. Med. Chem.*, 2005, vol. 20, p. 183.
35. Zanatta, N., Alues, S.H., Coelho, H.S., et al., *Bioorg. Med. Chem.,* 2007, vol. 15, p. 1947.